Journal of Geosciences, Osaka City University
Vol. 22, Art. 6, p. 151-166
March, 1979

Thermal Structure under the Ground in Osaka Plain, Southwest Japan

Koichi NAKAGAWA and Ken'ichi KOMATSU*

(with 3 Tables and 12 Figures)

1. Introduction

An information of the temperature distribution under the earth's surface is sometimes useful to interpret the complicated geophenomena. To determine the value of terrestrial heat flow precisely, the temperature gradient with depth and the thermal conductivity of the subsurface material of the ground are required to be measured. Since the thermal state in the ground near the surface is usually disturbed by atmospheric temperature change and transfer of under ground water, the borehole should be deep enough to obtain reliable temperature change with depth. The geothermal survey of the terrestrial heat flow in Japan Islands and its circumference sea was made by Uyeda and Horai (1964). They estimated thermal structure around Japan Islands based upon the measurements of temperature in the most of pre-Miocene basement strata.

However, little studies have been made so far on the geothermal characteristics of younger sediment on land. In the Osaka area, which is covered by the thick Post Pliocene sedimentary strata with thickness of several hundreds meters, about ten deep holes were available to obtain temperature distribution in the ground.

The average temperature gradient in the Post Pliocene strata in Osaka was found as about 2°C/100 meters. The apparent heat flow calculated based upon temperature gradient and thermal conductivity, however, shows some changes with depth. Generally, the heat flow in the lower strata below about 200 m are rather constant and larger compared with the upper strata.

This paper reports the results of geothermal survey in Osaka area and discusses the relationships between the terrestrial heat flow and geological conditions.

The authors wish to thank Dr. Michiji Tsurumaki, Prof. Taro Kasama, and Mr. Tsuneo Okuda for their hospitality and encouragement.

2. Measurement

The temperature distribution in the subsurface strata were measured at several boreholes and wells in Osaka Plain. The depth of the boreholes selected for this study

* Student at Osaka City University. (Present, Eengineer of Toa Nenryo Kogyo Co. Ltd.)

ranges from 250 to 900 meters. The thermal conductivities of the strata were estimated through laboratory test applied for undisturbed sediment samples as well as remolded samples.

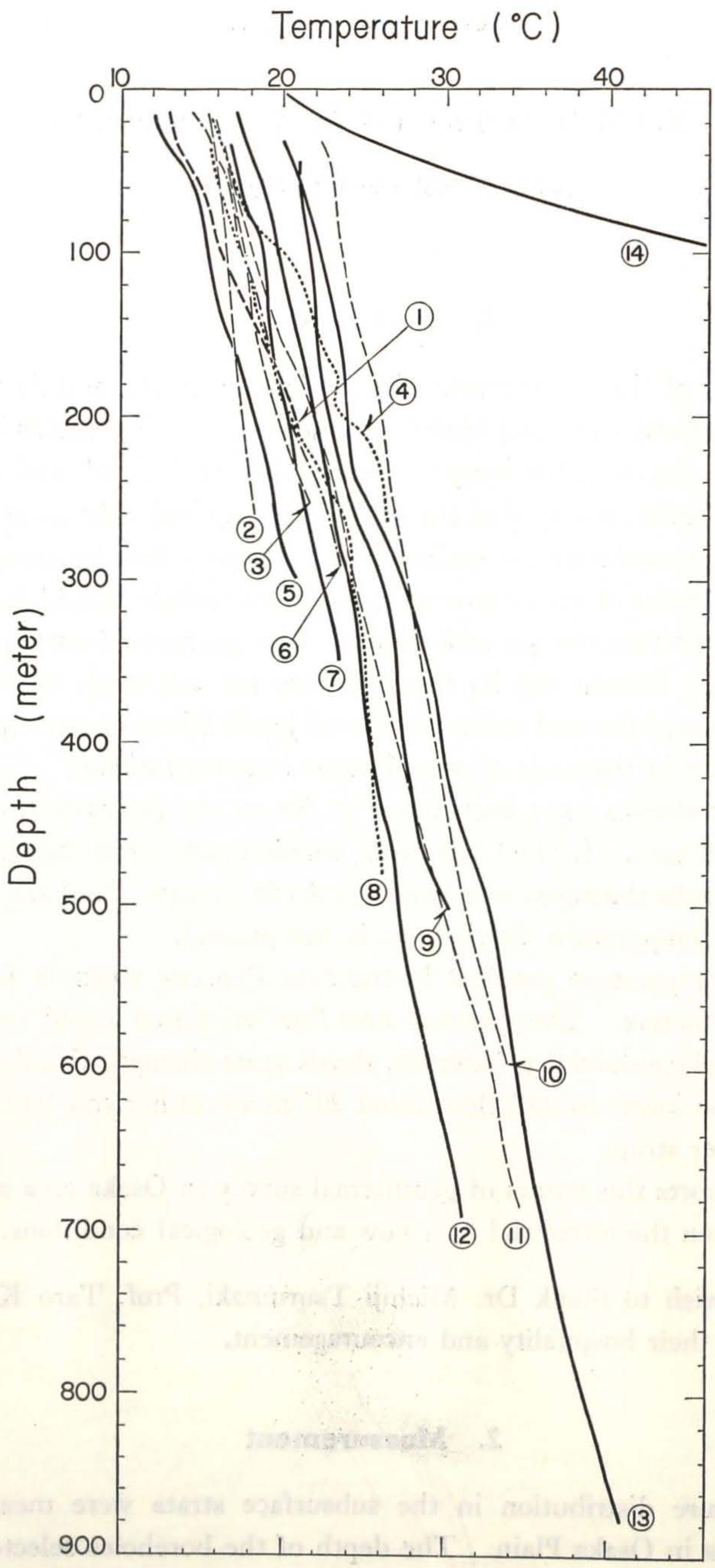

Fig. 1. Relation between temperature and depth. The numbers in the figure show the localities of observational station listed in Table 1.

Table 1. Locality measured, temperature, maximum depth and average geothermal gradient.

No.	Locality: Station	Latitude (N)	Longitude (E)	Maximum depth (m)	Geothermal Gradient (°C/100 m)	Remark*
1	Tarui, Sennan-Gun	34°22′	135°16′	200	4.22	
2	Kishiki-cho, Kishiwada C.	34°27′	135°22′	250	1.07	
3	Ooizumi, Sakai C.	34°34′	135°32′	250	2.45	
4	Ishizunishi, Sakai C.	34°34′	135°26′	270	4.85	
5	Isonokami, Kishiwada C.	34°29′	135°23′	300	3.13	
6	Minamishima, Sakai C.	34°36′	135°29′	300	3.05	
7	Torigai, Settsu C.	34°47′	135°35′	350	1.97	
8	Tikuko, Sakai C.	34°35′	135°25′	480	2.62	
9	Shindensakai, Daito C.	34°43′	135°37′	500	2.07	OD-6
10	Miyakojima, Osaka C.	34°42′	135°32′	670	2.06	OD-2
11	Mikuriya, Higashiosaka C.	34°40′	135°36′	700	1.62	OD-3
12	Tonouchi, Amagasaki C.	34°44′	135°28′	700	2.15	OD-5
13	Tanakamotomachi, Osaka C.	34°39′	135°27′	900	2.47	OD-1
14	Arima sp., Nishinomiya C.	34°47′	135°14′	450	19.3	

* Deep well's number

Geothermal gradient

Geothermal gradient $\Delta T/\Delta h$ were measured by thermister type thermometer with the precision of 0.1°C, where T and h are temperature and depth. The relation between temperature and depth is shown as in Fig. 1. The localities of observational station and summaries of measurement are listed in Table 1. The maximum depth in the present work was about 900 meters. Temperature gradients listed in Table 1 were calculated from temperature distribution near the bottom of each borehole.

Thermal conductivity

The most strata concerned with the present work consist of Post Pliocene sediments. Direct measurement of the thermal conductivity of the intact samples was not possible due to lack of the samples of the measured boreholes. The soil test data, however, were available and the boring log has been described for each borehole at the time of boring. Some soil samples were obtained from the measured boreholes and were used to measure the thermal conduvtivity as well as block samples. Conductivity of strata whose samples were not available, was estimated based upon the experimental relationship with appropriate physical characteristics.

For laboratory measurement of the thermal conductivity of the samples, divided bar technique as well as needle probe technique was used.

The divided bar technique applied to the samples of rocks and consolidated clayey

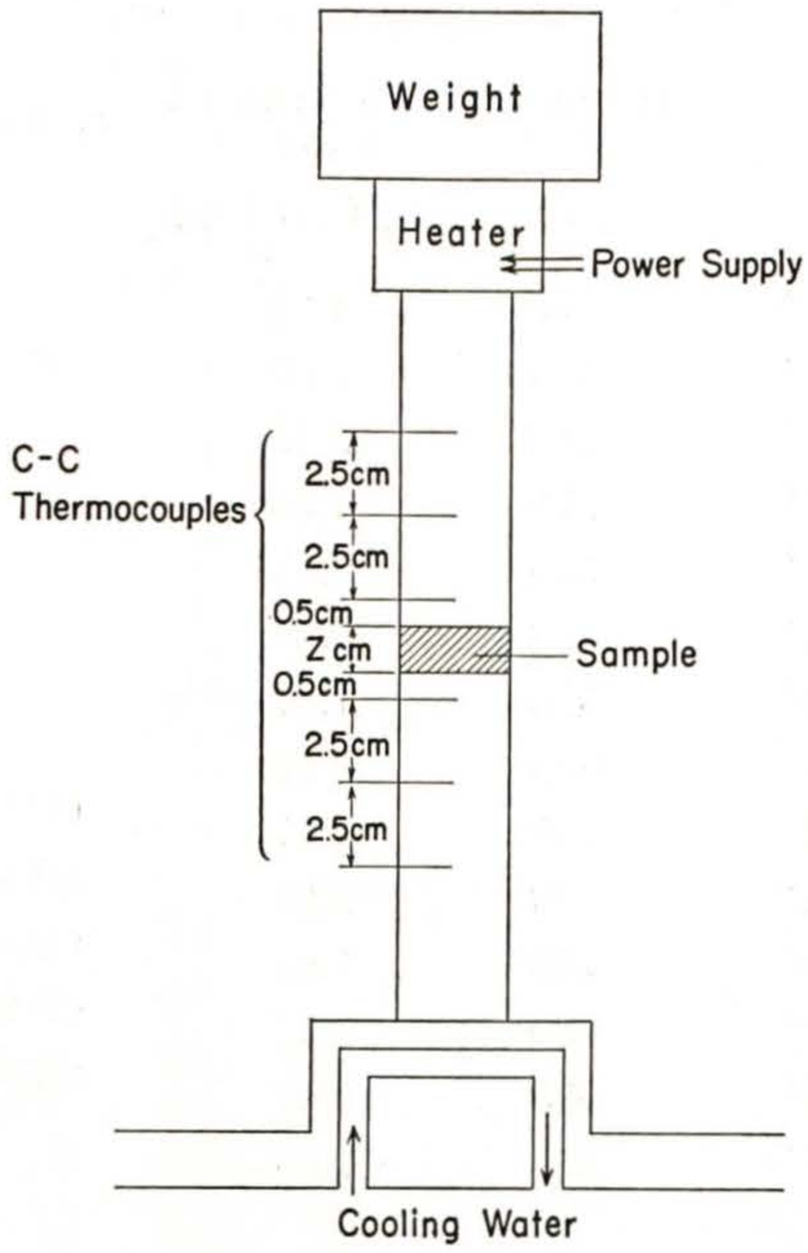

Fig. 2. Schematic diagram for apparatus of divided bar technique.

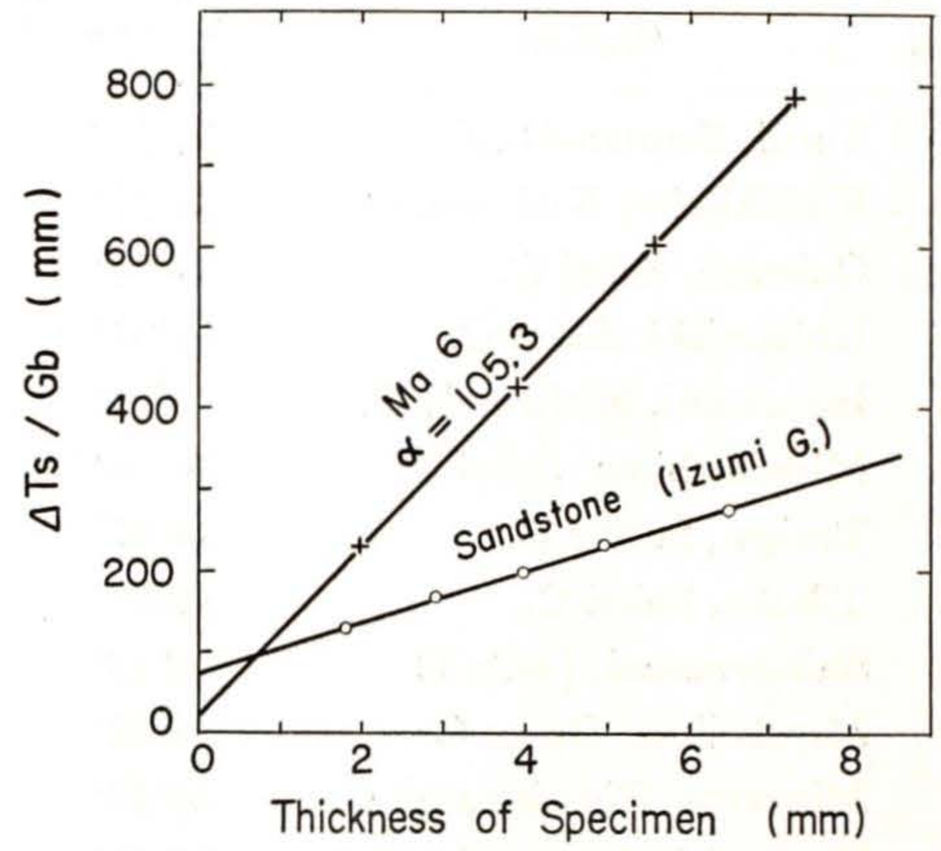

Fig. 3. The examples of relation between $\Delta T_s/G_b$ and thickness of sample, Z, obtained from divided bar technique.

sediments is basically similar to that of Horai (1959). Brass bar and sample, however, were protected by the sponge rubber foam, so that the temperature disturbance by air convection becomes to be minimized. Clayey samples with high water content were covered with the thin vinyl membrane to prevent desiccation. The schematic diagram of this technique used is shown in Fig. 2. It was found to take about three hours to reach steady state of the thermal flow in the system. After reaching steady state linear relationship between the difference of temperature at the ends of samples ΔT_s and thickness of the sample Z was obtained as shown in Fig. 3. Then,

$$\frac{\Delta T_s}{G_b} = \alpha Z + C \qquad \cdots\cdots (1)$$

where G_b is the temperature gradient in the brass, and α and C are constant. Thermal conductivity of sample K_s is calculated from a slope of straight line in the graph,

$$K_s = \frac{K_B}{\alpha} \qquad \cdots\cdots (2)$$

where K_B is thermal conductivity of brass bars.

The needle probe technique used to measure for soft sediments was reported by Herzen and Maxwell (1959). The schematic diagram of this apparatus is shown in Fig. 4. In this method, manganin wire and *C-C* thermocouples were used as heat generator and temperature sensor, respectively. The theoretical treatment for the needle

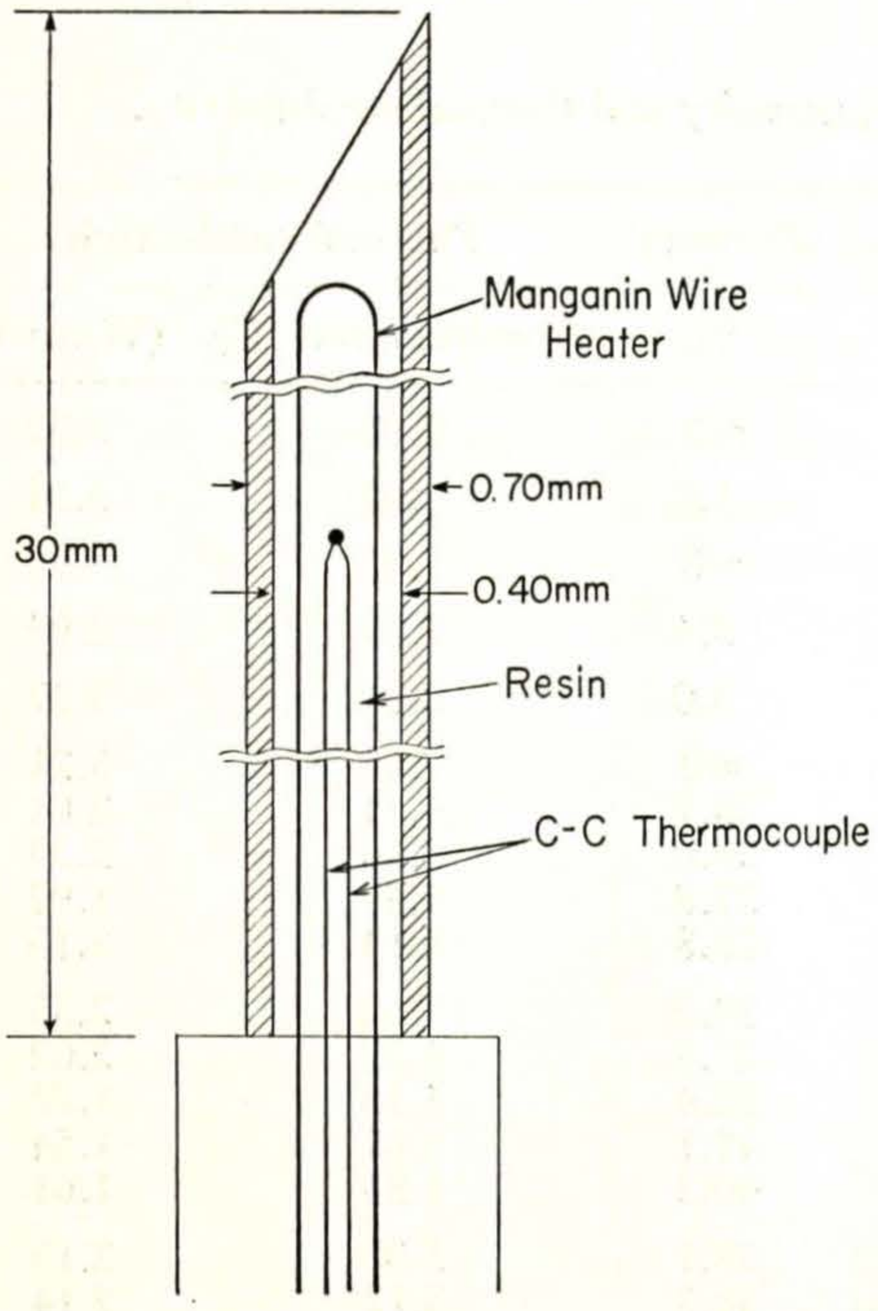

Fig. 4. Schematic diagram for apparatus of needle probe.

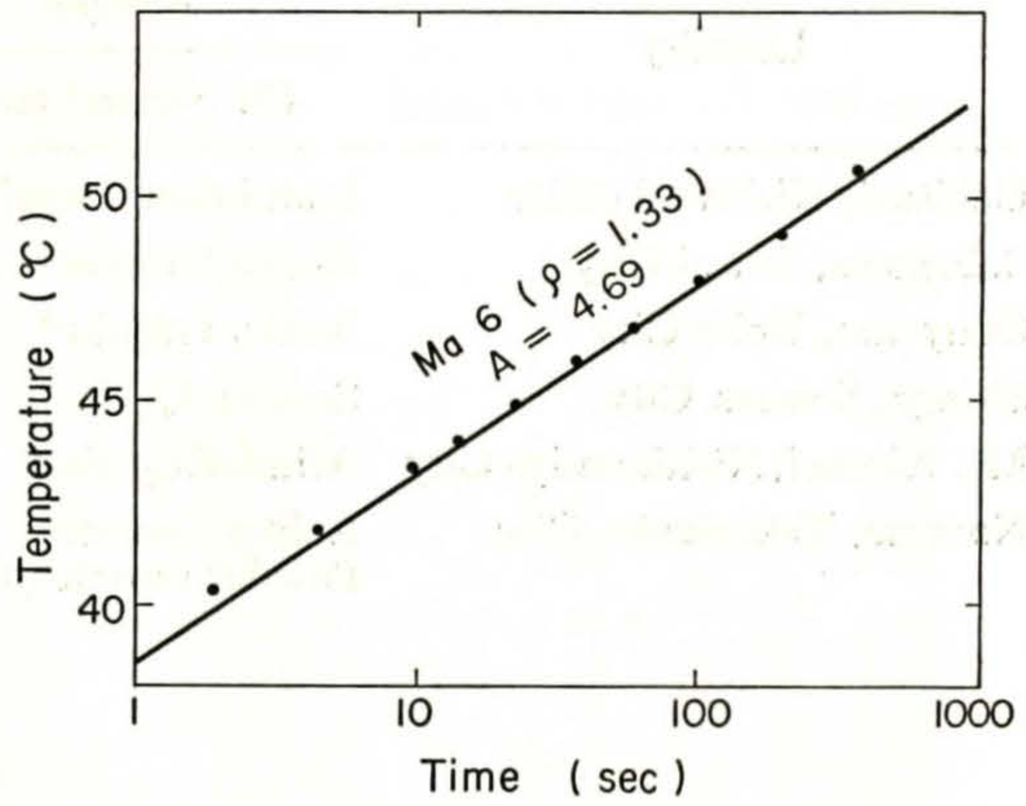

Fig. 5. An example of relation between the temperature rise and ln t obtained from needle probe technique (see the text).

probe technique to measure the thermal conductivity was developed by Jaeger (1956 and 1957). The relation between the temperature rise of probe with time is evaluated and approximately given by the following equation

$$T = \frac{Q}{4K_s} \ln \frac{4\kappa t}{AR} \qquad \text{.....(3)}$$

where

T : temperature rise
Q : generating heat per unit length per unit time
κ : thermal diffusivity
R : radius of probe
A : constant=1.7811

An example of relation between the temperature and ln t for a needle probe measurement of a soil sample, Ma 6, is shown in Fig. 5.

The values of thermal conductivity of soil sample obtained by these above two different techniques, agree with each other resulting in only several percents of the difference.

Samples are several kinds of rocks and sediments found in or near Osaka Plain, Southwest Japan. Rock samples are the Rokko granite, Ryoke granite, Sennan acidic rocks (quartz porphyry), Arima rhyolite, Izumi sandstone and Tanabe Group (mudstone). Sediments samples are clay, silt and sand of Osaka Group (the Pliocene and the Pleistocene) and the Recent.

Table 2. Description of the sampling locality, porosity and thermal conductivity.

Locality	Sample (*: Natural state)	Porosity %	Thermal conductivity (mcal/cm·sec·°C)	(W/m·°C)
Ushitaki, Kishiwada City	Izumi Sandstone*	≈0	8.05	3.37
Sobagawa, Izumi City	Ryoke Granite*	1.2	7.67	3.21
Okuyama, Kobe City	Rokko Granite*	≈0	7.93	3.32
Shinge, Sennan City	Sennan Q.P*.	3.4	7.07	2.96
Mt. Kinmei, Nishinomiya City	Arima Rhyolite*	3.0	8.06	3.37
Namaze, Takarazuka City	Rokko Granite*	≈0	7.66	3.21
	Powder sample (mix.)	28.7	4.81	2.01
		30.0	5.56	2.33
		27.8	4.59	1.92
		28.8	5.14	2.15
		29.2	5.62	2.35
		27.5	4.82	2.02
	(74μm~250μm)	38.4	4.10	1.72
	(250μm~420μm)	41.1	3.67	1.54
	(420μm~840μm)	40.3	3.85	1.61
Tanakamotomachi, Minato-ku, Osaka City	OD-1, Sand (<420μm)	38.1	5.08	2.13
	(<250μm)	38.3	5.12	2.14
		41.3	4.66	1.95
		40.6	5.01	2.10
		40.5	4.54	1.90
	(<1680μm)	41.2	3.90	1.63
	(840μm~1680μm)	41.6	3.72	1.62
		41.2	3.69	1.54
	(420μm~840μm)	41.5	3.88	1.69
		38.8	4.02	1.68
	(250μm~420μm)	39.4	4.02	1.68
		40.0	4.03	1.69
		41.5	4.57	1.91
	(74μm~250μm)	38.2	3.48	1.46
		38.5	3.39	1.84
		39.4	4.42	1.85
		41.2	3.61	1.51
		39.4	4.42	1.85
	(<74μm)	58.4	3.14	1.31
		61.3	2.82	1.18
Komyo-ike, Sakai City	Marine Clay, Ma 1*	54.0	3.22	1.35
		65.8	2.55	1.07
		82.9	1.97	0.82
	*	52.1	2.46	1.03
		55.2	2.52	1.06
		58.8	2.88	1.21
		63.0	2.34	0.98
		61.2	2.32	0.97
		60.6	2.52	1.06
		52.7	2.92	1.22
		63.3	2.66	1.11
		53.3	3.27	1.37

Table 2. continued

Locality	Sample (*: Natural state)	Porosity %	Thermal conductivity (mcal/cm·sec·°C)	(W/m·°C)
Kishiki-Cho, Kishiwda City	Marine Clay, Ma 3*	60.0	2.63	1.10
Tanabe, Wakayama Pref.	Mudstone (Tabnabe G.)*	15.2	5.41	2.26
Taishibashi, Osaka City	Marine Clay, Ma 6	80.0	2.07	0.87
		75.3	2.35	0.98
		62.4	2.62	1.10
		63.1	2.46	1.03
		63.1	2.48	1.04
		67.1	2.51	1.05
		76.1	2.28	0.95
		73.3	2.11	0.88
		77.1	1.98	0.83
		78.5	1.94	0.81
		79.1	1.87	0.78
		68.5	2.79	1.17
		68.7	2.94	1.23
		67.3	2.39	1.00
		67.3	3.19	1.34
		68.5	2.45	1.03
		68.5	2.07	0.87
		65.2	2.28	0.95
		67.3	2.13	0.89
		62.4	2.29	0.96
		54.8	2.68	1.12
		58.8	2.35	0.98
	*	61.5	2.96	1.24
Ashiya Coast Off	Marine Clay, Ma 10	65.6	2.43	1.02
		65.8	1.84	0.77
		59.4	2.94	1.23
		60.6	2.90	1.21
		57.6	2.78	1.16
		55.8	2.79	1.17
		63.6	2.39	1.00
	*	60.6	2.30	1.13
	*	55.8	2.97	1.24
	*	55.8	2.70	1.13
	Marin Clay, Ma 12*	65.0	2.60	1.09
	*	66.1	2.43	1.02
	*	65.7	2.37	0.99
	*	65.5	2.59	1.08
	*	65.7	2.14	0.90
	Silt	40.6	3.94	1.65
		43.0	3.62	1.52

The most sediment samples were measured under the both condition of undisturbed natural state and consolidated state after remolding. The Rokko granite was also measured as crushed powder sample with the particle size less than 74 microns. The brief description of those samples and the result of the thermal conductivity measurement are tabulated in Table 2.

3. Discussion

To determine the terrestrial heat flow, it is very important to estimate the thermal conductivity of the strata with reasonable accuracy. The thermal conductivity of sediments is found to depend upon such factors as mineral assemblage, fabric (including inter-particle bonding structure), porosity, composition and pressure of interstitial fluid, pressure, temperature and so on.

Horai and Baldridge (1971) examined experimentally the relation between thermal conductivity of rock and mineral composition, chemical composition (normative mineral composition) and mean atomic weight based upon rock samples. They concluded that the thermal conductivity of sedimentary rock or metamorphic rock can be estimated from mineral composition and porosity if they are macroscopically homogeneous and isotropic. Thermal conductivity of igneous rock is found to depend its chemical composition rather than mineral composition and porosity.

Woodside and Messmer (1961) gave the thermal conductivity of saturated mixture as following equation,

$$K_s = \exp\left[n \ln K_w + (1-n) \ln K_m\right] \quad \cdots\cdots\cdots\cdots\cdots\cdots\cdots\cdots\cdots\cdots (4)$$

where K_s, K_m and K_w are thermal conductivities of saturated mixture, mineral particle and water, respectively, and n is porosity of mixture which corresponds to volume fraction of water.

Horai and Simmon (1969) found the following relation to give good accuracy based upon their experimental result by the needle probe technique,

$$K_s = \frac{K_u + K_L}{2} \quad \cdots\cdots\cdots\cdots\cdots\cdots\cdots\cdots\cdots\cdots\cdots\cdots\cdots\cdots\cdots\cdots (5)$$

where K_u and K_L are upper and lower bounds of the thermal conductivity of mixture. This is arithmetic average of the upper and lower bounds of conductivity for a composite materials as a function of volumetric fractions and conductivities of constituent. The conductivities, K_u and K_L, have been carried out theoretically by Hashin and Shtrikman (1962) as following

$$K_u = K_m + \frac{n}{\dfrac{1}{K_w - K_m} + \dfrac{1-n}{3K_w}} \quad \cdots\cdots\cdots\cdots\cdots\cdots\cdots\cdots\cdots\cdots\cdots\cdots (6)$$

$$K_L = K_w + \frac{1-n}{\frac{1}{K_m - K_w} + \frac{n}{3K_w}} \quad \cdots\cdots(7)$$

The relation between thermal conductivity and porosity of rocks or sediments obtained by the authors is plotted in Fig. 6. The above equation (4) and (5) as well as an emperical equation by Bullard and Day (1961) which is

$$K_s^{-1} = 168 + 6.78w \quad \cdots\cdots(8)$$

are shown as solid lines in Fig. 6, where w is water content. The values of conductivities for mineral particle and water were assumed to be 8.45×10^{-3} cal/cm·sec·°C (3.54 w/m·°C) and 1.45×10^{-3} cal/cm·sec·°C, (0.607 w/m·°C) respectively. The assumed conductivity of mineral particle is an average value obtained from all granite in this work. As shown in Fig. 6, the fitting of plots and calculated curves are found rather satisfactory. This result may suggest that the main mother rock of sediments under Osaka Plain is considered to be the granitic rocks such as the Ryoke granite and the Rokko granite. These values

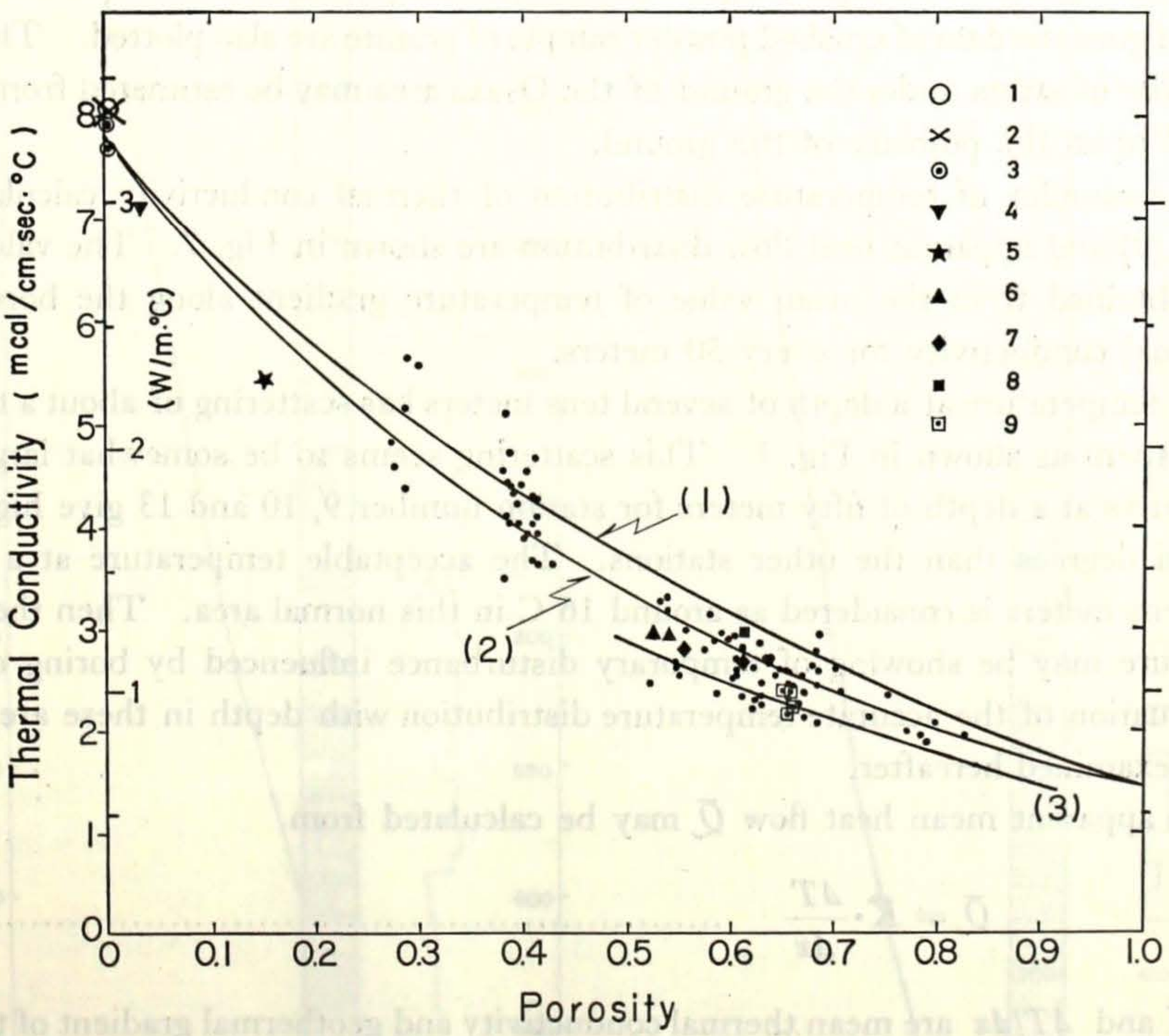

Fig. 6. Relation between thermal conductivity and porosity of saturated geomaterials sampled in the Osaka area. Symbol, 1: Rhyolite (Arima G.) 2: Sandstone (Izumi G.), 3: Granite (Rokko and Ryoke), 4: Quartz porphry (Sennan Acidic Rocks), 5: Mudstone (Tanabe G.), 6: Marine clay, Ma 1 (Osaka G.), 7: Marine clay, Ma 10 (Osaka G.), 8: Marine clay, Ma 6 (Osaka G.), 9: Marine clay, Ma 12 (Upper Pleistocene), which were measured in the natural state. The curves shown by solid line correspond to equations (10), (9) and (8) in the text, respectively.

of undisturbed natural clays are found slightly larger as compare with these of consolidated sample after remolding. This may be due to the difference of inter-particle bonding structure of clayey sediments. The difference of the thermal conductivities of clay under natural state and remolded state, however, is small as compared with the difference of the other mechanical properties like shear strength.

Using the equation (4) or (5), the thermal conductivity of the sediments in Osaka area may be estimated with reasonable accuracy with the error of the order of ten percents based upon the following equation, respectively,

$$K_m = \exp\{-(4.86+1.676n)\} \quad \text{.....(9)}$$

or

$$K_m = \frac{14.39+3.854n-9.2n^2}{1.856+3.38+n^2} \quad \text{.....(10)}$$

The value of thermal conductivity calculated from the equation (9) is smaller than (10) at an intermediate porosity range. As shown in Fig. 6, the experimental data of this work are found to be represented well by equation (9) rather than equation (10). In the same figure the data of crushed powder sample of granite are also plotted. The thermal conductivity of strata under the ground of the Osaka area may be estimated from equation (9) based upon the porosity of the ground.

The examples of temperature distribution of thermal conductivity calculated from equation (9) and apparent heat flow distribution are shown in Fig. 7. The value of heat flow is obtained from the mean value of temperature gradient along the borehole and the thermal conductivity for every 50 meters.

The temperature at a depth of several tens meters has scattering of about a ten degree between them as shown in Fig. 1. This scattering seems to be somewhat larger. The temperatures at a depth of fifty meters for station number 9, 10 and 13 give higher value of several degrees than the other stations. The acceptable temperature at a depth of several tens meters is considered as around 16°C in this normal area. Then these higher temperature may be showing of temporary disturbance influenced by boring operation. The evaluation of the accurate temperature distribution with depth in these areas should be more examined hereafter.

The apparent mean heat flow $\bar{Q}$ may be calculated from

$$\bar{Q} = \bar{K} \cdot \frac{\Delta T}{\Delta z} \quad \text{.....(11)}$$

where $\bar{K}$ and $\Delta T/\Delta z$ are mean thermal conductivity and geothermal gradient of the strata. The vertical distributions of apparent heat flow calculated for twelve holes are shown in Fig. 8. As shown in this figure, the value of heat flow are not constant with depth. The results of heat flow obtained are found that these values at ground surface are lower than those at deeper depth. The difference of the heat flow in the upper and lower strata may be interpreted as only changes of the atmospheric temperature or weather. Any

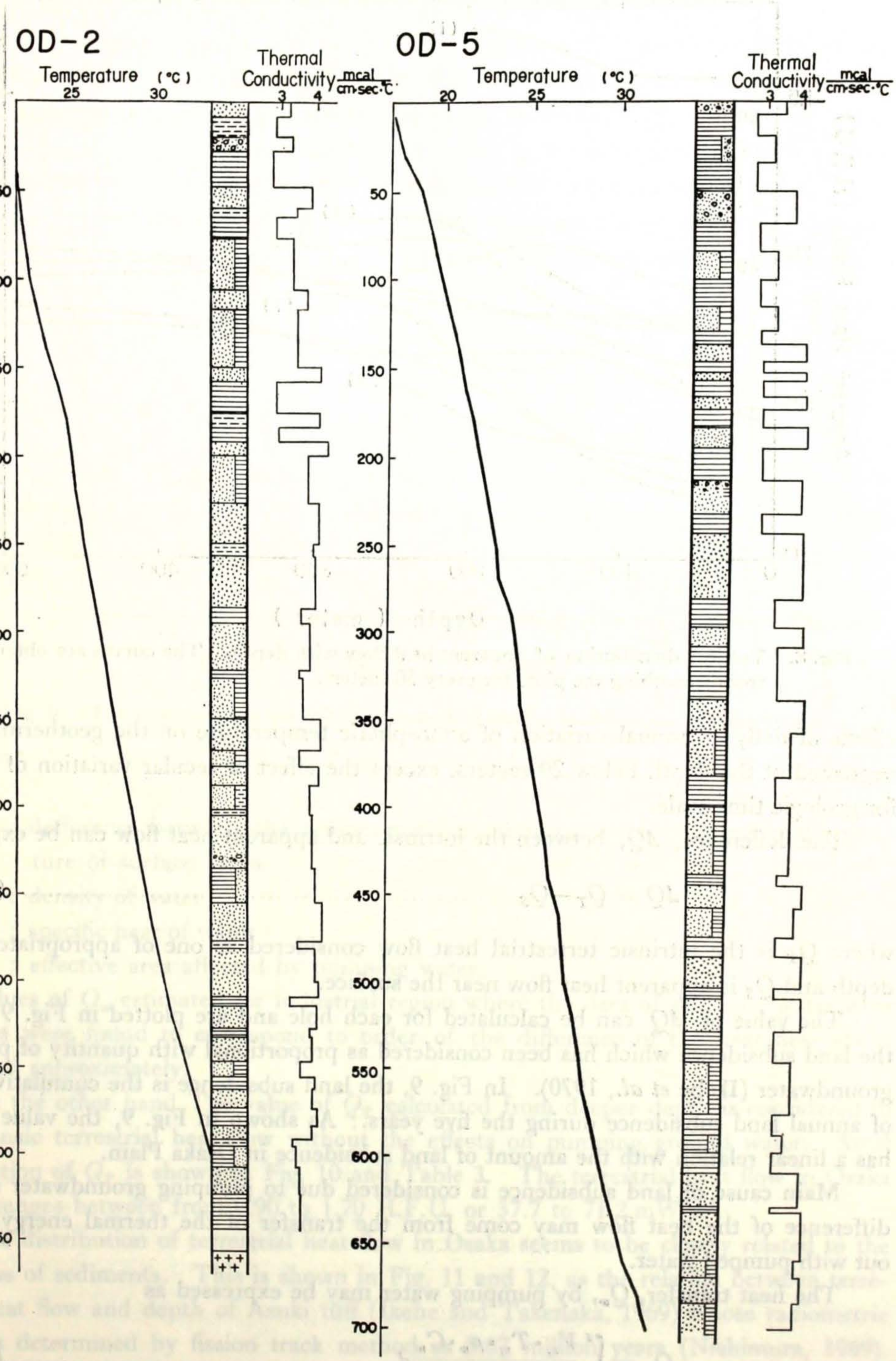

Fig. 7. Examples of temperature distribution and thermal conductivity distribution with depth. These localities are shown in Table 1.

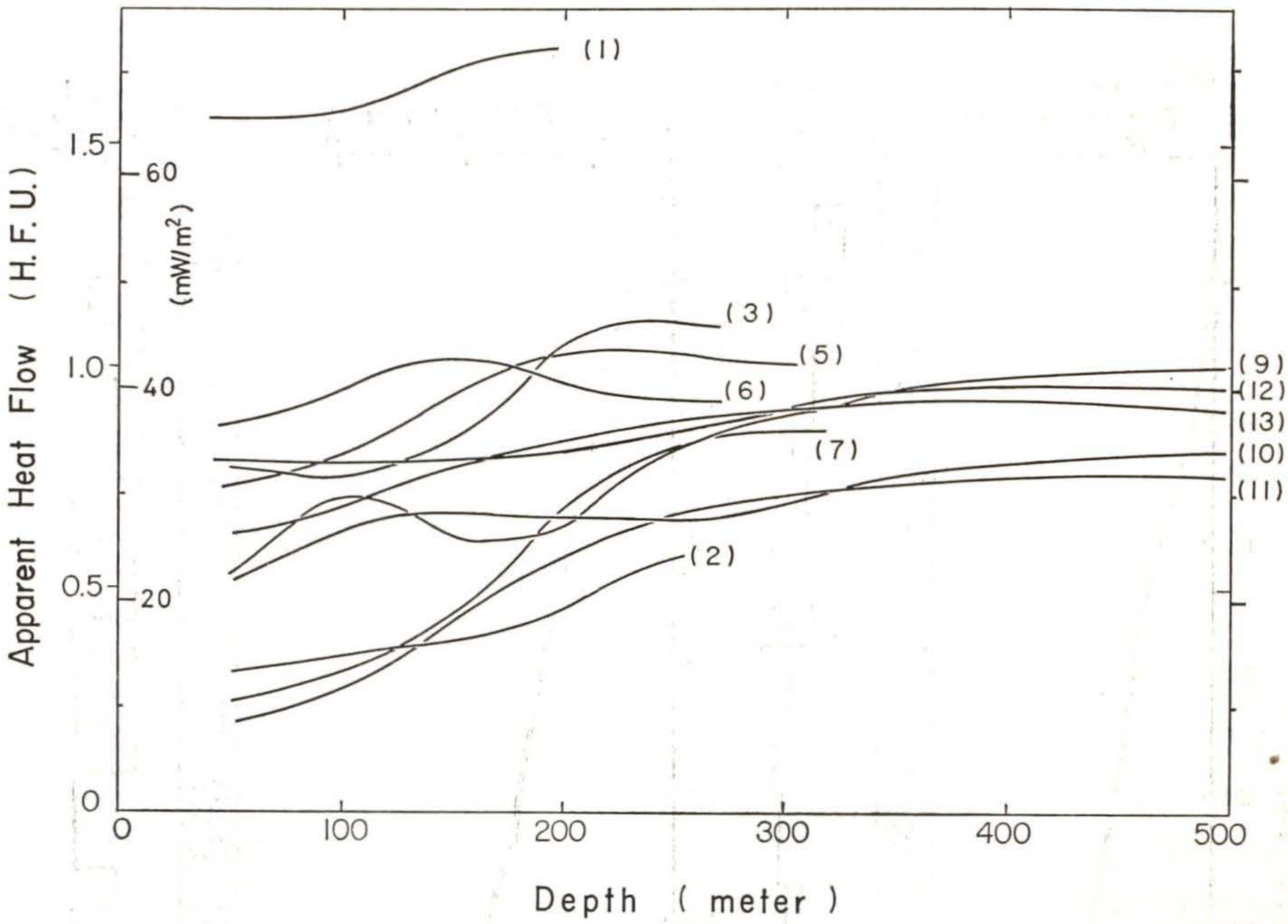

Fig. 8. Vertical distribution of apparent heat flow with depth. The curves are obtained from smoothing the plots for every 50 meters.

effects of daily or annual variation of atmospheric temperature on the geotherm can be negrected at the depth below 20 meters, except the effect of secular variation of crimate for geologic time scale.

The defference, ΔQ, between the intrinsic and apparent heat flow can be express as

$$\Delta Q = Q_T - Q_S \quad \cdots\cdots(12)$$

where Q_T is the intrinsic terrestrial heat flow considered as one of appropriate deeper depth and Q_S is apparent heat flow near the surface.

The value of ΔQ can be calculated for each hole and are plotted in Fig. 9 against the land subsidence which has been considered as proportional with quantity of pumping groundwater (Ikebe *et al.*, 1970). In Fig. 9, the land subsidence is the cumulative value of annual land subsidence during the five years. As shown in Fig. 9, the value of ΔQ has a linear relation with the amount of land subsidence in Osaka Plain.

Main cause of land subsidence is considered due to pumping groundwater and the difference of the heat flow may come from the transfer of the thermal energy carried out with pumped water.

The heat transfer, Q_w, by pumping water may be expressed as

$$Q_w = \int_0^z \frac{V_{z_i} \cdot T_{z_i} \cdot \rho_w \cdot C_w}{S} d_z \quad \cdots\cdots(13)$$

V_{z_i} : water volume per unit time by pumping out from the depth of z

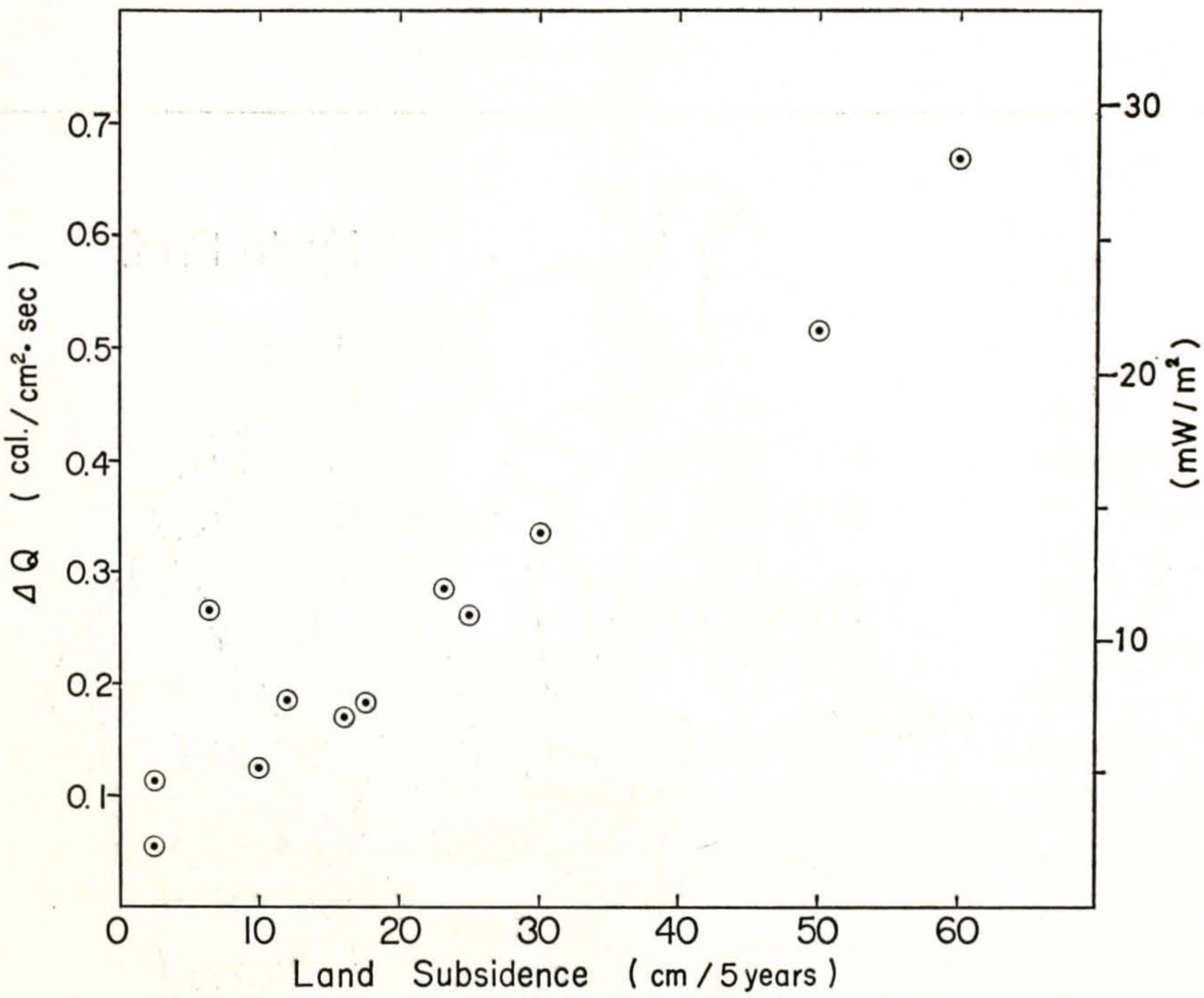

Fig. 9. The relation between ΔQ and amount of land subsidence during five years.

T_{z_i} : defference between the temperature of pumping water and mean temperature of surface flows

ρ_w : density of water

C_w : specific heat of water

S : effective area affected by pumping water.

Values of Q_w estimated for industrial region where the data of pumping water were obtained were found to correspond to order of the difference of the heat flow above described approximately.

On the other hand The value of Q_T calculated from deeper depth is considered to be intrinsic terrestrial heat flow without the effects on pumping ground water. Areal distribution of Q_T is shown in Fig. 10 and Table 3. The terrestrial heat flow in Osaka region ranges between from 0.90 to 1.70 H.F.U. or 37.7 to 71.2 mW/m².

The distribution of terrestrial heat flow in Osaka seems to be closely related to the thickness of sediments. This is shown in Fig. 11 and 12, as the relation between terrestrial heat flow and depth of Azuki tuff (Ikebe and Takenaka, 1969) whose radiometric age was determined by fission track method as 0.87 million years (Nishimura, 1969). From these fact, the areal distribution of terrestrial heat flow in Osaka may be concluded as consistent with the Post Pliocene tectonic structure.

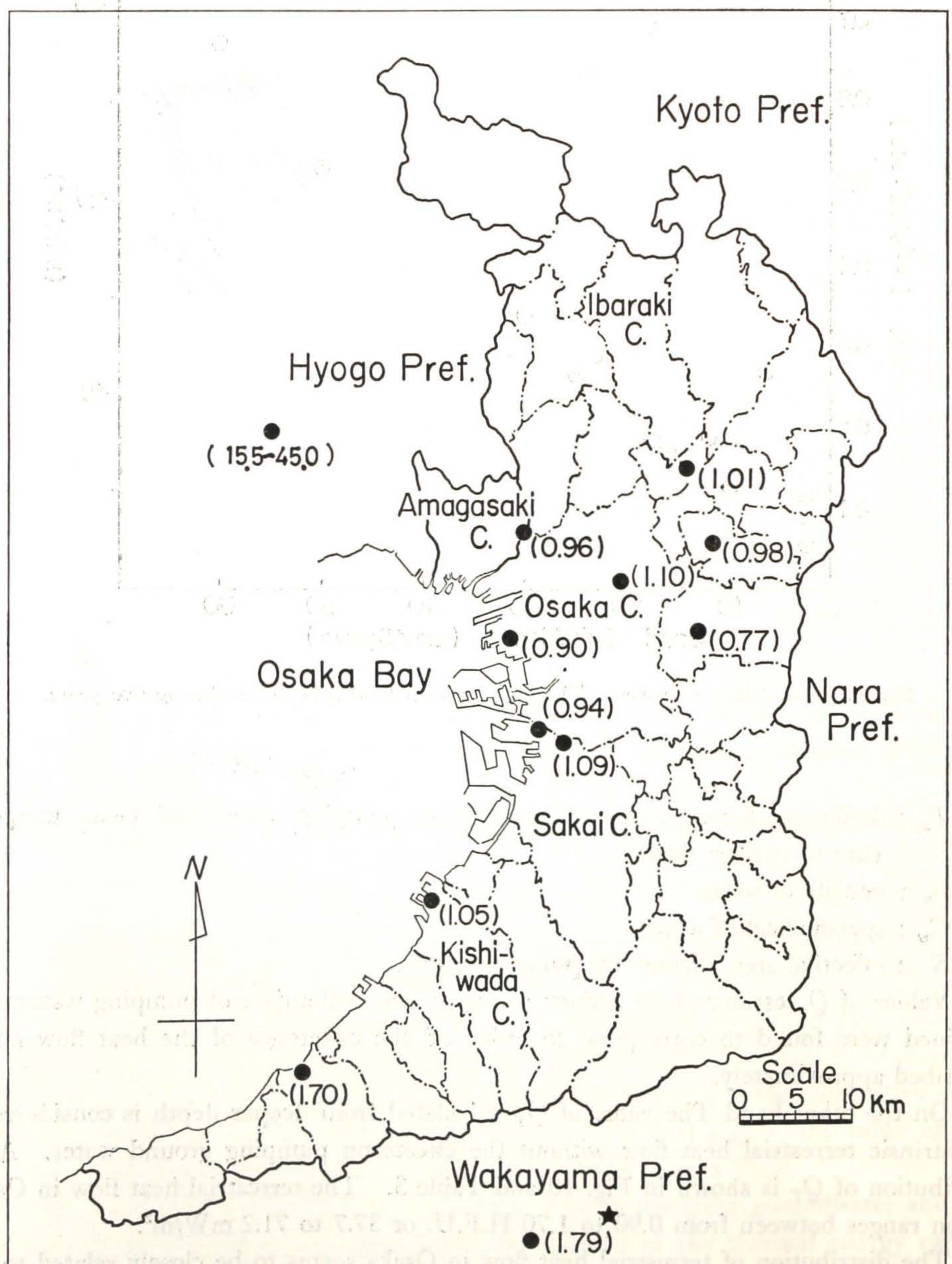

Fig. 10. The areal distribution of terrestrial heat flow (H.F.U.) in Osaka Plain. Asterisked value was obtained by Uyeda and Horai (1969).

Table 3. Terrestrial heat flow in Osaka.

Lacality		Heat Flow*			
No.	Station	(H.F.U.)		mW/m	
1	Tarui, Sennan-Gun	1.70		71.2	
3	Ooizumi, Sakai C.	1.09		45.6	
4	Isonokami, Kishiwada C.	1.05		44.0	
5	Minamishima, Sakai C.	0.94		39.4	
7	Torigai, Settsu C.	1 01		42.4	
9	Shindensakai, Daito C.	0.98	(1.16)	41.0	(48.6)
10	Miyakojima, Osaka C.	1.10	(1 13)	46.1	(47.3)
11	Mikuriya, Higashiosaka C.	0.77		32.2	
12	Tonouchi, Amagasaki C.	0.96		40.2	
13	Tanakamotomachi, Osaka C.	0.90	(1.00)	37.7	(46.1)
14	Arima sp., Nishinomiya C.	15.5 ≀ 45 0		649 ≀ 1,884	

* Parenthesized ralues were obtained from the average conductivity and the geothermal gradient which was calculated from temperature supposed as 16°C at a depth of 50 meters and temperature at the bottom of hole.

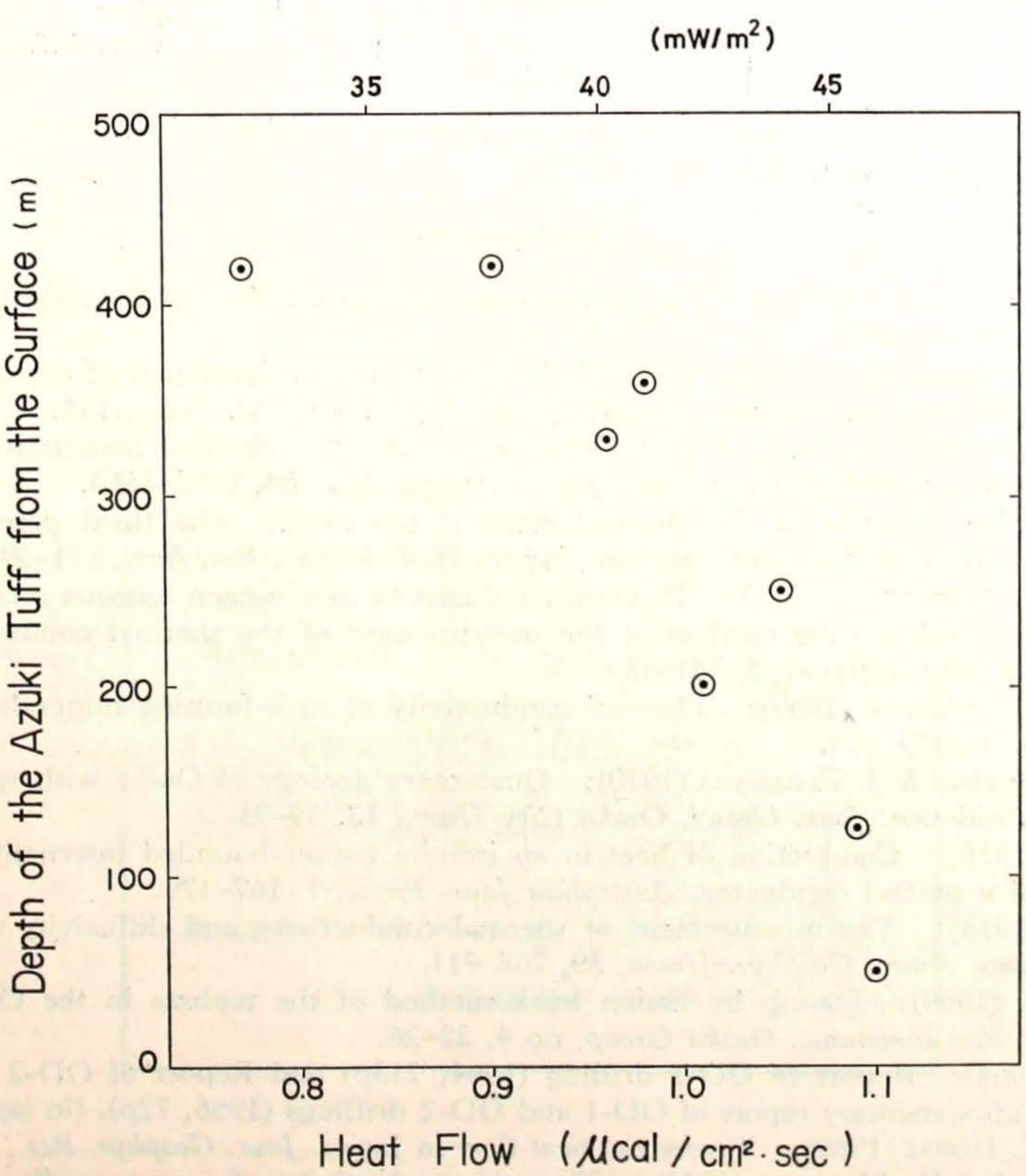

Fig. 11. Relation between terrestrial heat flow and depth of Azuki Tuff. The depth of Azuki Tuff is estimated from Ikebe *et al.* (1970).

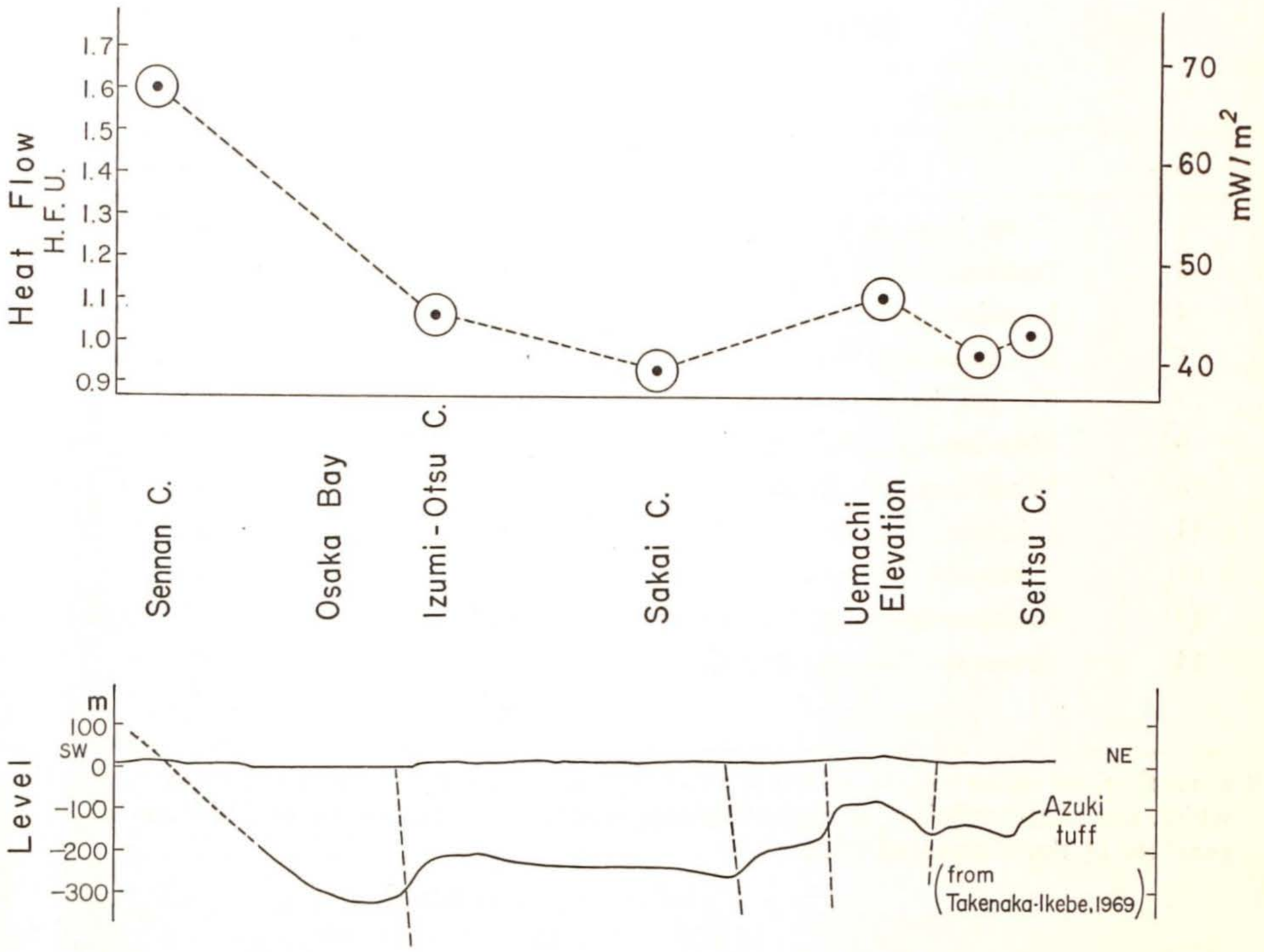

Fig. 12. The SW-NE section of Osaka Plain showing the relation between terrestrial heat flow and depth of Azuki Tuff.

References

BULLARD, E.C. & A. DAY (1961): The flow of heat through the floor of the Atlantic Ocean. *Geophys. Jour.*, **4**, 282–292.

HASHIN Z. & S. SHTRIKMAN (1962): A variational approach to the theory of the effective magnetic permeability of multiphase materials. *Jour. Appl. Phys.*, **33,** 3125–3131.

HERZEN R.V. & A.E. MAXWELL (1959): The measurement of thermal conductivity of deep-sea sediments by a needle probe method. *Jour. Geophys. Res.*, **64,** 1557–1563.

HORAI K. (1959): Studies of the thermal state of the earth. The third paper: Terrestrial heat flow at Hitachi, Ibaragi Prefecture, Japan. *Bull. Earthq. Res. Inst.*, 571–591.

HORAI K. & S. BALDRIDGE (1971): Thermal conductivity of nineteen igneous rocks I. Appreciation of the needle probe method to the measurement of the thermal conductivity of rock. *Phys. Earth Plan. Interiors,* **5,** 151–156.

HORAI K. & G. SIMMON (1969): Thermal conductivity of rock-forming minerals. *Earth Planet. Sci. Letters*, **6,** 359–368.

IKEBE, N., J. IWATSU & J. TAKENAKA (1970): Quaternary geology of Osaka with special reference to land subsidence. *Jour. Geosci. Osaka City Univ.*, **13,** 39–95.

JAEGER, J.C. (1956): Conduction of heat in an infinite region bounded internally by a circular cylinder of a perfect conductor. *Australian Jour. Phys.*, **9,** 167–179.

JAEGER, J.C. (1958): The measurement of thermal conductivity and diffusivity with cylindrical probe. *Trans. Amer. Geophys. Union,* **39,** 708–711.

NISHIMURA, S. (1969): Dating by fission track method of the tephras in the Osaka group (in Japanese). *Res. communic. Osaka Group,* no 4, 22–26.

Osaka City (1964): Report of OD-1 drilling (1964, 213p) and Report of OD-2 drilling (1965, 152p). Supplementary report of OD-1 and OD-2 drillings (1966, 72p). (in japanease).

UYEDA S. & K. HORAI (1969): Terrestrial heat flow in Japan. *Jour. Geophys. Res.*, **69,** 2121–2141.

WOODSIDE W. & J.H. MESSMER (1961): Thermal conductivity of porous media, 1. *Jour. Appl. Phys.*, **32,** 1688–1699.